# A SOLAR-FLUX TEMPERATURE RELATIONSHIP DERIVED FROM MULTIPLE-SATELLITE ORBITAL DECAY

**Doyle T. Hall[(1)], Phillip Anz-Meador[(2)]**

*[(1)]Hernandez Engineering Inc., 2400 NASA Road 1 - Mail Code C-104, Johnson Space Center, Houston TX 77058, Email: Doyle.T.Hall1@jsc.nasa.gov*
*[(2)] Viking Science and Technology, 16821 Buccaneer Lane, Suite 216, Houston TX 77058, Email: panz-meador@vsti.com*

## ABSTRACT

We report an analysis of the orbital decay rates of 95 satellites to determine the best-fit relationship between solar 10.7cm flux ($F_{10.7cm}$) and Earth's globally-averaged exospheric temperature ($T_\infty$). The analysis focuses on reproducing atmospheric drag rates observed over a period spanning nearly 3 solar cycles, and yields globally-averaged exospheric temperatures appropriate for use in models that project Earth's satellite and orbital debris populations many decades into the future. Exospheric temperatures derived using an oblate-Earth/rotating atmosphere drag model are uniformly larger than best-fit temperatures derived using a spherical-Earth/non-rotating atmosphere model, an effect that should be included in long-term orbital debris projection models.

## 1. INTRODUCTION

Atmospheric drag significantly affects the orbits of satellites and orbital debris in low-Earth orbit ultimately causing many to plunge into the atmosphere and a fiery end. Radar observations of satellite trajectories clearly reveal that orbital semi-major axes typically decrease slowly early in a satellite's orbital lifetime, and then more rapidly as the orbit decays into the thicker regions of the atmosphere. Several parameters govern orbital decay rates, including the satellite's drag coefficient and area-to-mass ratio as well as the terrestrial exospheric temperature [1]. The exospheric temperature is a measure of the heat balance in the uppermost region of Earth's atmosphere, where molecular collisions are infrequent, and where heating is dominated by absorption of extreme-ultraviolet (EUV) solar photons and supplemented by auroral energy-deposition (see [2] and [3] and references therein).

Spatial variations in exospheric temperature include a local-time asymmetry (temperatures typically peak in the mid-afternoon) and localized enhancements over Earth's polar regions, especially large during times of intense auroral activity [2 and 3]. While such spatial asymmetries are important in determining short-term variations in satellite decay rates (i.e., with time scales less than a few days), the goal of this analysis is to provide a computationally efficient means of estimating decay rates averaged over much longer time scales, as required when projecting orbital debris populations many decades into the future. Such long-term decay can be estimated by neglecting spatial variations, and using a single globally-averaged exospheric temperature ($T_\infty$), a quantity that varies mostly in response to changes in solar EUV flux [2, 3 and 4]. Although solar EUV output is not observable from Earth's surface, space-based observations indicate that it correlates very strongly with the solar 10.7cm flux ($F_{10.7cm}$), which has been measured by ground-based observatories for several decades [4].

We report an analysis of the orbital decay rates of 95 satellites (observed between years 1962 and 2000) to determine the best-fit relationship between $F_{10.7cm}$ and $T_\infty$. Two basic classes of satellites are included in the study. The first comprises 44 satellites that have known shapes and masses and, thus, well determined area-to-mass ratios. Satellites in the second class do not have known area-to-mass ratios, but are included because they orbited for more than 22 years before reentering the atmosphere. The 51 satellites in this class each had an orbital lifetime that spanned more than two 11-year solar activity cycles, and each traversed both high- and low-altitude regions of the upper atmosphere. Together, these two satellite classes constitute a data set particularly relevant in determining long-term, globally-averaged exospheric temperature variations. Best-fit exospheric temperature parameters are generated for two types of atmospheric drag model: an *oblate-Earth/rotating* model which calculates drag rates accounting for the effects of planetary oblateness and the tendency for the Earth's atmosphere to rotate once per day, and a *spherical-Earth/non-rotating* model that neglects both oblateness and atmospheric rotation.

*Proceedings of the 3rd European Conference on Space Debris, ESOC, Darmstadt, Germany, 19 - 21 March 2001*
*(ESA SP-473, August 2001)*

## 2. MODELING SATELLITE ORBITAL DECAY RATES

Radar observations obtained by the United States Space Command Space Surveillance Network (SSN) provide direct measurements of the satellite positions and orbital decay rates. Fig. 1 shows variations in semi-major axis, *a*, for SSN 2909 (one of the satellites used in this study) and illustrates the strong correlation of decay rates with solar 10.7cm flux. In this analysis, we determine globally-averaged exospheric temperatures that reproduce (in a best-fit sense) the combined orbital decay histories of 95 such satellites.

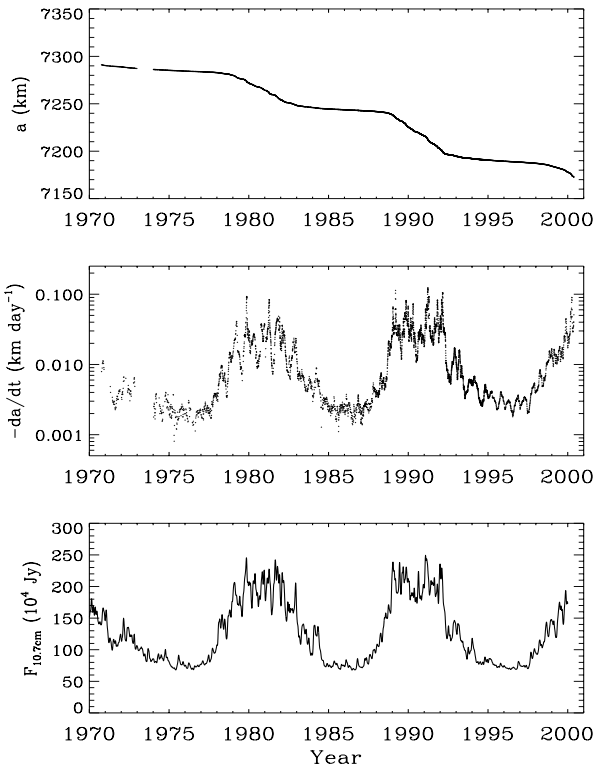


Fig. 1. Semi-major axis history for SSN 2909, one of 95 satellites used in the analysis.

### 2.1 Satellite Orbital Decay Observations

Satellites included in this analysis belong to two basic classes. The 44 satellites in the first class have known shapes and masses and, thus, well-determined area-to-mass ratios. This set includes 17 perfectly spherical satellites, and 27 cylindrical rocket-bodies. Area-to-mass ratios for these satellites (tabulated in [5]) are used as input parameters in the best-fit analysis. The 51 satellites in the second class do not have known area-to-mass ratios, but were selected because each had an orbital lifetime that spanned more than 22 years (i.e., more than two 11-year solar activity cycles) before reentering the atmosphere. The area-to-mass ratios for these satellites are determined as part of the best-fit analysis using techniques similar to those used in previous studies (see [5]).

SSN two-line element (TLE) sets obtained from the archive at Johnson Space Center are used to calculate estimates of time derivatives of semi-major axes throughout the orbital histories of each satellite. These time derivatives and their associated uncertainties comprise a set

$$\{\dot{a}_{j,k}, \sigma_{j,k}, t_{j,k}\} \qquad (1)$$

where the index *j* denotes the satellite number (*j=1…95*) and the index *k* denotes the measurement number obtained at time $t_{j,k}$. Each derivative and associated uncertainty is estimated numerically using TLE observations measured within $t_{j,k} \pm 15$ days, and each thus represents an average over a ≈30-day period. Fig. 1 (middle panel) shows the time derivatives calculated in this manner, as well as the solar 10.7cm flux also averaged over a 30-day period (bottom panel). The combined data from the 95 satellites constitute 273,000 semi-major axis derivative measurements, obtained during the years 1962 through 2000 spanning perigee altitudes from 200km up to 1000km.

### 2.2 Model Orbital Decay Rates

The expression for the time-derivative of a satellite's semi-major axis (*averaged over one orbital period*) may be written

$$\dot{a}(\vec{E},t) = \left(A/m\right)\left[C_D F(\vec{E},t) + C_R G(\vec{E},t)\right] \qquad (2)$$

where *F* is a function that expresses atmospheric drag perturbations (see [1] for a detailed description), *G* expresses solar radiation pressure perturbations (see [6] and [7]; note that *G* vanishes unless the orbit of the satellite traverses Earth's shadow, and is generally much smaller than *F*). Because Eq. 2 expresses the rate averaged over one orbital period, *F* and *G* depend on the first five Keplerian orbital elements of the satellite, denoted here as

$$\vec{E} = (a, e, i, \omega, \Omega). \qquad (3)$$

The functions *F* and *G* also depend on time, *t*, through dependencies on variable atmospheric and solar flux parameters.

As indicated in Eq. 2, atmospheric drag and solar

proportional to *A/m*, the ratio of the satellite's aspect-averaged cross sectional area to its total mass. The quantities $C_D$ and $C_R$ denote the satellite's drag coefficient and net-reflectance coefficient respectively. Drag coefficients are assumed to be $C_D = 2.2$ for all satellites at all altitudes. Reflectance coefficients are similarly taken to be $C_R = 1.0$ in all cases, although the results of the analysis are very insensitive to this choice, and change insignificantly over the entire permittable range of $0.0 \le C_R \le 2.0$.

In order to optimize the match between observed and modeled orbital decay rates, a goodness-of-fit indicator is defined as follows:

$$\chi^2 = \sum_{j,k} \left[ \frac{\dot{a}_{j,k} - \dot{a}(\vec{E}_{j,k}, t_{j,k})}{\sigma_{j,k}} \right]^2 . \qquad (4)$$

Minimizing this quantity with respect to the unknown parameters yields the best-fit solution.

### 2.3 Atmospheric Models

The drag-rate function, *F*, in Eq. 2 is linearly proportional to the atmospheric mass density at satellite perigee, and depends on the atmospheric scale height at perigee as well (see [1] for a detailed discussion). Because the Earth has an oblate figure (its polar radius is ≈20km smaller than its equatorial radius), perigee altitudes are latitude-dependent, an effect often neglected in drag-rate calculations. In this analysis we consider two different atmospheric models. The first *oblate-Earth/rotating* model includes the effects of Earth's oblateness and also assumes that the atmosphere rotates once per day. The second, less realistic (but much more computationally efficient) *spherical-Earth/non-rotating* model neglects both oblateness and atmospheric rotation (see [1] for a detailed discussion of oblateness and atmospheric rotation on orbital decay rates). As discussed below, best-fit exospheric temperatures for these two models differ.

The vertical structure of the atmosphere is specified using the atmospheric mass density, ρ, a function of altitude, *z*, and the exospheric temperature:

$$\rho = \rho(z, T_\infty). \qquad (5)$$

The atmospheric scale height can be expressed similarly. Atmospheric densities and scale heights are taken from the Jacchia (1977) tabulation [2].

## 3. EXOSPHERIC TEMPERATURES FOR LONG-TERM ORBITAL PROJECTIONS

As discussed previously, projecting satellite and orbital debris populations many decades into the future demands a computationally efficient method of estimating atmospheric drag rates. Previous studies of orbital decay that have included spatial as well as short-term temporal exospheric variations, incorporate both the solar 10.7cm flux and geomagnetic indices (*Kp* or *Ap*) as predictors of exospheric temperature [2]. However, including such variations in long-term orbital debris projections would be computationally prohibitive, as it would require orbital integration time steps much shorter than satellite orbital periods. In order to permit longer time steps, many orbital projection models neglect spatial variations in exospheric temperatures altogether, and use a single global value averaged over time scales much longer than individual satellite orbital periods. The objective of this analysis is to derive best-fit exospheric temperatures to be used in such long-term projection models.

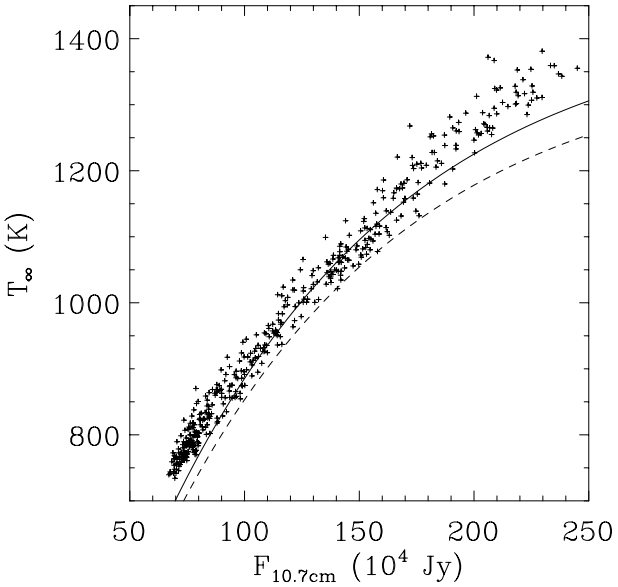


Fig. 1. Globally-averaged exospheric temperatures. The + symbols show monthly averages from the Jacchia (1977) formulation [2]. The solid and dashed lines show best-fit results for the oblate-Earth/rotating atmosphere model and the spherical-Earth/non-rotating atmospheric model respectively.

### 3.1 Temperature/Solar Flux Relationship

To achieve the goal of computational efficiency for long-term projections we neglect variations in geomagnetic indices, and model atmospheric drag rates using a simple relationship between globally-averaged

$$T_\infty = T_o \left[1 - e^{-\nu F_{10.7cm}}\right], \qquad (6)$$

where $T_o$ and $\nu$ are free parameters determined in the best-fit analysis. Solar 10.7cm fluxes are averaged over the same time span used to determine the semi-major axis derivatives, 30-days for this analysis (see section 2.1). Determining the best-fit values for $T_o$ and $\nu$ involves minimizing the goodness-of-fit indicator given in Eq. 4, using the numerical minimization techniques described in [9].

The relationship given in Eq. 6 was applied previously to the decay of the LDEF satellite, which orbited from 1984 through 1990 [8]; the analysis used a spherical-Earth/non-rotating atmospheric model and yielded best-fit values $T_o$ = (1314.1 ± 35.1) K and $\nu$ = (11.16 ± 0.82) × $10^{-7}$ $Jy^{-1}$. When the current analysis procedure is similarly applied to the LDEF satellite data, it yields best-fit values $T_o$ = (1323.4 ± 21.8) K and $\nu$ = (10.65 ± 0.30) × $10^{-7}$ $Jy^{-1}$, which overlap the previous analysis results at the 1-$\sigma$ level of uncertainty.

### 3.2 Best-fit Results and Conclusions

Best-fit coefficients determined using the complete 95-satellite data set are $T_o$ = (1437 ± 28) K and $\nu$ = (9.57 ± 0.18) × $10^{-7}$ $Jy^{-1}$ for the oblate-Earth/rotating atmosphere model, and $T_o$ = (1378 ± 22) K and $\nu$ = (9.65 ± 0.18) × $10^{-7}$ $Jy^{-1}$ for the spherical-Earth/non-rotating model. Fig. 2 shows the best-fit relationships. For comparison, Fig. 2 also shows globally- and monthly-averaged exospheric temperatures calculated using the Jacchia (1977) formulation [2], which includes estimated contributions from both solar flux and geomagnetic variations.

At times of enhanced solar activity (i.e., when $F_{10.7cm}$ $\tau$ 200 × $10^4$ Jy) the current analysis (using the oblate-Earth/rotating atmospheric model) yields noticeably cooler exospheric temperatures than the Jacchia (1977) formulation. This is not surprising, however, because the Jacchia (1977) exospheric temperature formulation was developed using satellite decay rates observed primarily at low-to-moderate solar activity levels [2], while the more extensive data set used in this analysis spans nearly three solar cycles and samples all activity levels. The difference suggests that the Jacchia (1977) model, as originally formulated, may overestimate rates of atmospheric drag at times near maximum solar activity.

The analysis also indicates exospheric temperatures used in orbital projection models that employ the spherical-Earth/non-rotating approximation need to be cooler on average than in models that account for Earth's oblateness and rotating atmosphere. This difference is driven by the fact that, given the same vertical atmospheric structure, the spherical/non-rotating atmosphere approximation predicts higher average rates of orbital decay relative to the more realistic oblate/rotating model. In order for each atmospheric drag model to match the rates of orbital decay observed for actual satellites, the exospheric temperatures must differ by about 30K to 50K, as is apparent in Fig 2. Ideally, this effect should be included in long-term orbital projection models that employ the spherical/non-rotating atmosphere approximation.

## 4. REFERENCES


1. King-Hele D., *Satellite Orbits in an Atmosphere: Theory and Applications*, Blackie, London, 1987.

2. Jacchia L. G., *Thermospheric Temperature, Density and Composition: New Models*, Smithsonian Astrophysical Observatory Special Report 375, 1977.

3. Hedin A. E., The Atmospheric Model in the Region 90 to 2000km, *Adv. Space Res.*, Vol. 8, No. 5, 9-25, 1988.

4. Lean, J., Solar EUV Irradiances and Indices, *Adv. Space Res.*, Vol. 8, No. 5, 263-292, 1988.

5. Reynolds R. C. et al., *NASA Standard Breakup Model 1998 Revision*, Lockheed Martin Houston, LMSMSS-32532, 1998.

6. Vallado D. A., *Fundamentals of Astrodynamics and Applications*, McGraw Hill Co., New York, 1997.

7. Roy A. E., *Orbital Motion (3rd Edition)*, Adam Hilger, Bristol , 1988.

8. Badwhar G. D., Exospheric Temperatures During Solar Cycle 22, *J. Astronaut. Sciences*, Vol. 38, 369-375.

9. Press W. H. et al., *Numerical Recipes in FORTRAN 77 (2nd Ed.)*, Cambridge Univ. Press, Cambridge, 1992.